Published in final edited form as:

Curr Biol. 2022 December 05; 32(23): 5031–5044.e4. doi:10.1016/j.cub.2022.10.015.

Cell types and molecular architecture of the *Octopus bimaculoides* visual system

Jeremea O. Songco-Casey[1], **Gabrielle C. Coffing**[2], **Denise M. Piscopo**[1], **Judit R. Pungor**[1], **Andrew D. Kern**[2], **Adam C. Miller**[1], **Cristopher M. Niell**[1,3,4,*]

[1]Institute of Neuroscience, University of Oregon, Eugene, OR 97403, USA

[2]Institute of Ecology and Evolution, University of Oregon, Eugene, OR 97403, USA

[3]Twitter: @cris_niell

[4]Lead contact

SUMMARY

Cephalopods have a remarkable visual system, with a camera-type eye and high acuity vision that they use for a wide range of sophisticated visually driven behaviors. However, the cephalopod brain is organized dramatically differently from that of vertebrates and invertebrates, and beyond neuroanatomical descriptions, little is known regarding the cell types and molecular determinants of their visual system organization. Here, we present a comprehensive single-cell molecular atlas of the octopus optic lobe, which is the primary visual processing structure in the cephalopod brain. We combined single-cell RNA sequencing with RNA fluorescence *in situ* hybridization to both identify putative molecular cell types and determine their anatomical and spatial organization within the optic lobe. Our results reveal six major neuronal cell classes identified by neurotransmitter/neuropeptide usage, in addition to non-neuronal and immature neuronal populations. We find that additional markers divide these neuronal classes into subtypes with distinct anatomical localizations, revealing further diversity and a detailed laminar organization within the optic lobe. We also delineate the immature neurons within this continuously growing tissue into subtypes defined by evolutionarily conserved developmental genes as well as novel cephalopod- and octopus-specific genes. Together, these findings outline the organizational

*Correspondence: cniell@uoregon.edu.

AUTHOR CONTRIBUTIONS

C.M.N. and A.C.M. conceived and oversaw the project. J.O.S.-C., D.M.P., and J.R.P. collected sequencing data. G.C.C. and A.D.K. performed genome assembly and annotation; J.R.P. performed cross-species gene identification; and J.O.S.-C., A.C.M., and C.M.N. performed scRNA-seq analysis. J.O.S.-C. and D.M.P. performed FISH experiments. All authors contributed to writing and editing of the manuscript.

SUPPLEMENTAL INFORMATION

Supplemental information can be found online at https://doi.org/10.1016/j.cub.2022.10.015.

DECLARATION OF INTERESTS

The authors declare no competing interests.

INCLUSION AND DIVERSITY

One or more of the authors of this paper self-identifies as an underrepresented ethnic minority in their field of research within their geographical location. One or more of the authors of this paper self-identifies as a member of the LGBTQIA+ community. One or more of the authors of this paper received support from a program designed to increase minority representation in their field of research. When citing references scientifically relevant for this work, we also actively worked to promote gender balance in our reference list. We support inclusive, diverse, and equitable conduct of research.

logic of the octopus visual system, based on functional determinants, laminar identity, and developmental markers/pathways. The resulting atlas presented here details the “parts list” for neural circuits used for vision in octopus, providing a platform for investigations into the development and function of the octopus visual system as well as the evolution of visual processing.

In brief

Songco-Casey et al. combine scRNA-seq and RNA FISH to characterize molecular cell types in the octopus visual system. Cell classes are delineated by neurotransmitters/neuropeptides and additional functional or developmental markers, revealing both sublayer organization of the optic lobe and immature neurons that correspond to mature cell types.

Graphical Abstract

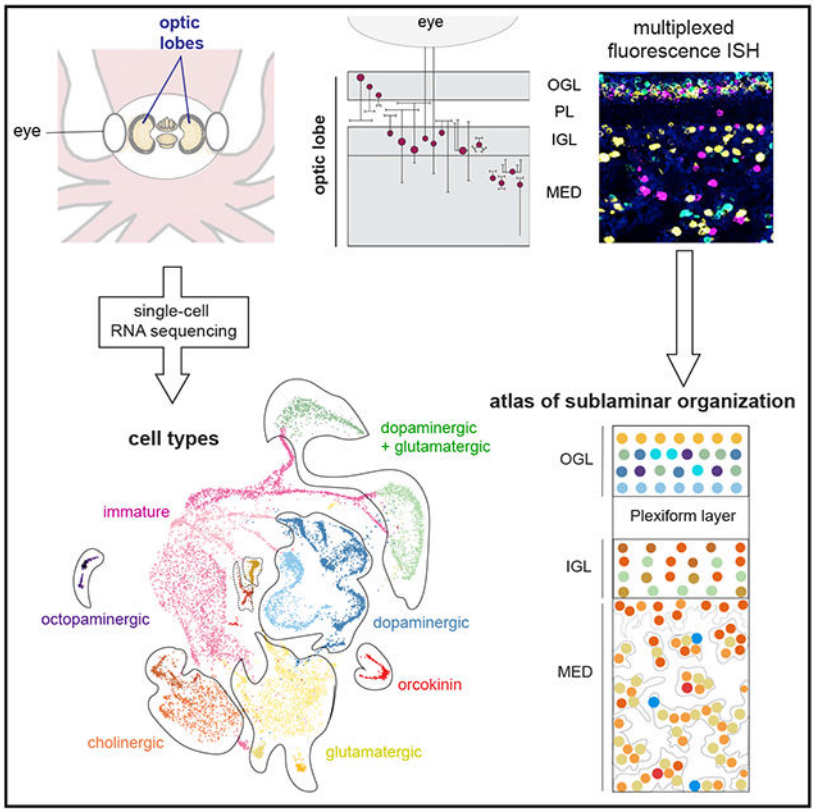

INTRODUCTION

Cephalopods represent a unique branch of the animal kingdom for studying vision. Coleoid cephalopods (octopuses, squids, and cuttlefish) have the largest brain among invertebrates,[1–3] much of which is composed of areas dedicated to visual processing: the optic lobes.[4,5] Their visual system facilitates a range of behaviors such as navigation, prey capture, and complex camouflage.[1,6–8] However, the neural basis of central visual processing in cephalopods is largely unknown.

Despite diverging over 500 million years ago, octopuses independently evolved camera-type eyes similar to those of vertebrates.[9] However, the neural organization of structures that process visual information is dramatically different in the two lineages. In contrast to the vertebrate retina, which is an intricate neural circuit with a diversity of cell types, the octopus retina consists only of photoreceptors and supporting cells.[10,11] The photoreceptors send axons into the central brain, targeting the optic lobes that lie directly behind the eyes[10] (Figure 1A). The optic lobes, which make up approximately two-thirds of the octopus' central brain,[12,13] are where the bulk of visual processing is hypothesized to occur.[12–14] Optic lobe outputs project to deeper brain regions, including those involved in learning/memory and motor behavior.[12,15–19]

Histological studies by Young[5] have provided a description of the optic lobe's anatomical organization and neuronal morphologies (Figures 1B–1D), which we briefly summarize here. The outermost region of the optic lobe is a cell body layer, termed the outer granular layer (OGL). The OGL contains cells traditionally referred to as amacrine cells based on their morphology,[18,20] which have multipolar processes that ramify within the plexiform layer (PL) below the OGL. The PL is a dense neuropil and is the primary termination site of photoreceptor axons, optic lobe neuronal processes, and projections from deeper brain regions.[12,20] Below the PL is another cell body layer, the inner granular layer (IGL), which has a varied population including (1) neurons with bipolar morphology, (2) neurons that send centrifugal axons back to the retina, and (3) neurons of amacrine morphology with processes in the PL.[12,18] Finally, a deeper structure termed the medulla comprises the bulk of the optic lobe. The cells within the medulla are organized in a branching tree-like fashion which, in cross-section, appear as islands of cell bodies surrounded by neuropil.[21] The superficial region of the medulla is organized into columns and is referred to as the outer radial columnar zone, whereas the deeper region of the medulla includes processes that extend tangentially and is termed the central tangential zone.[5] Given the anatomical organization, it has been hypothesized that the outer layers of the optic lobe (OGL, PL, and IGL) may perform similar functions to the vertebrate retina, leading it to be termed the "deep retina,"[22] whereas the medulla may engage in higher order processing analogous to central visual areas in other species.[12]

Although the anatomy of these cell classes suggests an organizational foundation, fully understanding the neural circuitry necessitates knowledge of the molecular identities of these cell types, including both functional determinants (e.g., neurotransmitter and receptor repertoires) and developmental determinants (e.g., transcription factors and adhesion molecules). Recent molecular taxonomies in other species have provided new insight into the circuit organization of a number of brain regions including the fly visual system,[23] the mouse and primate retina,[24,25] and the mouse visual cortex.[26] We therefore sought to create a systematic molecular characterization of the octopus visual system by combining single-cell RNA sequencing (scRNA-seq), to determine transcriptional cell types, with multiplexed RNA fluorescence *in situ* hybridization (FISH), to determine the location of these cell types within the optic lobe.

RESULTS

scRNA-seq of the octopus optic lobe

We performed scRNA-seq in juvenile (1.5 months of age) *Octopus bimaculoides*. Despite their continued growth throughout their lifetime (1–2 years), the overall body organization, behavior, and visual system of *O. bimaculoides* are mature by this age,[27,28] allowing us to identify neural circuitry involved in a fully functioning, yet still growing, visual system. We performed Chromium 10x sequencing of cells from the optic lobes of two animals, processed separately as biological replicates, and aligned reads to an updated genome assembly and gene annotation using CellRanger (method details; Figure S1; Table S1).

A robust scRNA-seq analysis requires a contiguous genome with accurate, full-length gene annotations. The first genome assembly of *O. bimaculoides* (Octopus_bimaculoides_v2_0) is broken into over 150,000 scaffolds, with many split or truncated gene annotations. Alignment of our single-cell reads to this genome therefore resulted in low mapping. To resolve this, we used single molecule high fidelity (HiFi) sequencing to create a new contig level genome assembly and combined new Iso-Seq reads with existing bulk RNA-seq data to generate an improved genome annotation (method details; Figure S1; Table S1) containing 5,437 contigs and 18,896 gene annotations. The new assembly is more contiguous and helped lengthen the 3′ ends of many annotated genes, capturing more reads (Figure S1) and thus achieving higher resolution.

Using standard filtering, normalization, integration, and clustering in Seurat,[29,30] we identified a total of 28,855 cells across two biological replicates. Our analysis resulted in a total of 41 clusters, where each sample contributed cells to all of the identified clusters in similar proportions, supporting the reproducibility of this approach (Figure S2).

We first sought to broadly characterize the identified clusters in terms of neuronal and non-neuronal populations (Figure S3). We used a homologous sequence identifier, OrthoFinder,[31] to assign gene-family and orthology relationships using genes from *Drosophila*, vertebrates, and other cephalopod species (method details; Figure S3A for example gene trees). Genes that were not assigned to orthology groups by OrthoFinder were manually annotated using NCBI BLAST[32] if possible. Throughout, we name the octopus genes according to their assigned identity: e.g., synaptotagmin (*syt*), as summarized in Table S2, although we note that these assignments may be improved as our understanding of gene homology in cephalopods advances.

We expected a large proportion of the cells to have high expression of genes related to mature neurons, as well as potentially developing neurons, as the octopus brain continues to grow and add neurons throughout its lifetime.[33] To identify neurons within our scRNA-seq data, we first looked at the expression of genes related to synaptic vesicle release. We found that most clusters (33/41) expressed the *O. bimaculoides* SNARE genes, whereas only seven were likely to be non-neuronal, based on the absence of expression of these markers (Figure S3). The non-neuronal clusters represented ~8% of the cells and had relatively high expression of genes falling within gene families with functions consistent with proliferation, blood, endothelium, and glia (Figure S3). We used FISH to localize

expression of non-neuronal genes and found several to be primarily expressed outside of the optic lobe (see Figure S3 for further characterization). We therefore removed these clusters from subsequent analyses that aimed to delineate neuronal cell types, which included a total of 26,092 cells across 33 clusters.

To further explore the potential neural cell-type classes within the scRNA-seq clusters, we first examined the expression patterns of markers for neurotransmitter usage (Figure 2). Previous work identified dopamine, glutamate, and acetylcholine as the primary neurotransmitters used in the cephalopod optic lobe[34]; hence, we looked for standard markers of these neurotransmitter types based on their biosynthetic and vesicular packaging pathways (dopamine transporter [*dat*], vesicular glutamate transporter [*slc17a7*, or *vglut*], vesicular acetylcholine transporter [*slc18a3*, or *vacht*], and choline acetyltransferase [*chat*]) (Figures 2B, 2C, and S4). In addition, we identified a gene in the solute carrier gene superfamily (*slc6a15/18*), which acts to support glutamate synthesis via transport of glutamate precursors[35] and was closely co-expressed with *vglut* in both scRNA-seq data (Figure 2C) and FISH (Figure S4). We used *slc6a15/18* as an additional marker of glutamatergic neurons along with *vglut*, since, despite strong FISH signal, we found a relatively low number of scRNA-seq reads aligned to *vglut*, which may be due to an incomplete gene model for this gene.

Together, scRNA-seq expression of neurotransmitter markers delineated the majority of putative neurons (22/33 clusters) into four broad classes defined by either unique or combinatorial expression of these genes (Figures 2B and 2C). Each of these broad categories consisted of a number of unique clusters (Figures 2A and 2C), suggesting further cell-type heterogeneity within. In addition, two smaller neuronal clusters were identified, one of which did not express markers for any neurotransmitters, but did express the neuropeptide orcokinin (*orc*) (Figure 2B) and another that expressed a combination of *dat* and a marker for octopamine synthesis, tyramine beta-hydroxylase (*tyrbh*), previously identified in octopus optic lobe neurons.[36] We did not find a significant population of GABAergic neurons (based on expression of glutamate decarboxylase [*gad*]; Figure 2C), consistent with previous findings of the minimal role of GABA in the optic lobe.[37]

Finally, we found a large population of cells (9 clusters) that appear to be immature neurons, based on higher expression levels of early neural specification genes (i.e., embryonic lethal abnormal vision [*elav*] and CUG triplet repeat RNA binding protein [*celf*]), lower levels of genes involved in synaptic transmission, and no expression of any neurotransmitter markers (Figures 2C and S3). As described below, this class of cells expressed a diversity of evolutionarily conserved developmental genes and distinct subgroups had expression profiles suggestive of a relationship to distinct mature cell clusters.

Taken together, these findings support the idea that the scRNA-seq data captured expression profiles of unique classes of mature and immature neurons in the optic lobe. We used these data to delineate molecular cell types and assign them to an anatomical organization within the octopus optic lobe.

A molecular and spatial taxonomy of mature neural cell types

Our scRNA-seq data show that neurotransmitter usage divides the majority of octopus optic lobe neurons into four large classes–dopaminergic, dopaminergic+glutamatergic, glutamatergic, and cholinergic neurons–along with two smaller classes that utilize orcokinin or octopamine. To examine the localization of the four major neurotransmitter cell classes within the optic lobe, we performed FISH for *dat, slc6a15/18*, and *vacht* (Figure 3). Each of these neurotransmitter markers showed a distinct pattern of expression within the cell body layers of the OGL, IGL, and medulla (Figure 3B). Dopaminergic (*dat*+) cells were found predominantly in the OGL, with sparser expression in the IGL and medulla. Glutamatergic cells (*slc6a15/18*+; *vglut* in Figure S4) were found across the optic lobe, including in some *dat*+ cells in the OGL and IGL. Cholinergic cells (*vacht*+; *chat* in Figure S4) were restricted to the IGL and the medulla. As suggested by the scRNA-seq data (Figure 3A), glutamatergic and cholinergic neurons are segregated in their spatial expression patterns—both are expressed in non-overlapping cells in the IGL and medulla, with *slc6a15/18*+ expressed more strongly in the tangential region of the medulla and *vacht*+ expressed more strongly in the radial columnar region (Figure 3B). These mappings confirm that the scRNA-seq data identified distinct populations of neurons that correlate with distinct anatomical spatial expression patterns.

Within each of the large neurotransmitter-defined populations, further transcriptional heterogeneity was present, suggesting that the clusters within these populations may correspond to neuronal subtypes (Figure 2). We sought to determine if such cell types, as identified by their unique gene expression profiles, would occupy distinct anatomical locations within the optic lobe.

Dopaminergic neurons—In the scRNA-seq data, dopaminergic neurons spanned seven clusters (Figure 2), and *dat*+-only neurons were predominantly localized to the OGL (Figure 3B). We examined gene expression across *dat*+ clusters and found two subgroups defined by the complementary expression of either the homeobox transcription factor *six4/5* (clusters 12–17) or the neuropeptide *fmrf* (clusters 10–11) (Figure 4A). Across model species, the *six* family of genes are key regulators in head development,[38] eye specification, and retinal determination.[39–41] *fmrf* neuropeptides are known to regulate a variety of functions in mollusks,[42] including reproduction[43] and chromatophore control.[44,45] FISH revealed that within the *dat*+ cells in the OGL, the *six4/5*+ population represented a broad sublayer of neurons in the middle of the OGL, whereas *fmrf* expression corresponded to a sublayer of neurons deeper in the OGL, along the border of the PL. Thus, the *dat*+-only cells contain two subtypes that are differentiated by expression of a homeobox transcription factor and a neuropeptide, respectively. Notably, these are mainly localized within the OGL and hence likely represent a subset of the amacrine neurons of Young's anatomical classifications.[5]

Expression heterogeneity of additional genes suggested these two dopaminergic cell groups can be further subdivided. The clusters within the *six4/5*+ group differentially express several genes encoding neuropeptides (*pxfv*, *lxgkr*, and *flri*) which are largely non-overlapping, although FISH reveals a low level of co-expression (Figures 4A and 7D). This set of neuropeptides is particularly interesting as they were manually assigned

identities based on repetitive protein sequences, but there is little information regarding their function in other organisms, let alone cephalopods. Furthermore, a subset of cells within the *fmrf*+ group expresses the adhesion molecular *dscam*, which has been shown to mediate cell-type-specific self-avoidance among dopaminergic amacrine cells[46] and sublayer-specific connectivity in amacrine and bipolar cells[47] in the vertebrate retina. *dscam*+ cells form a discrete narrow band along the deep border of the OGL and the PL (Figure 4A), suggesting *dscam* could play a role in assigning their sublayer specificity. Together, these data demonstrate further heterogeneity within dopaminergic cell types in the OGL, identifying laminar organization from the superficial-to-deep layers.

Dopaminergic + glutamatergic neurons—Based on the co-expression of *dat* and *slc6a15/18* in both the scRNA-seq and FISH data, we sought to further delineate this cell class. The scRNA-seq clusters with overlapping *dat* and *slc6a15/18* expression suggested that two prominent groups, clusters 5/6 and 37, might correspond to subtypes. Furthermore, the expression of *dat* and *slc6a15/18* significantly overlapped in both the OGL and IGL, suggesting that these two locations might correspond to the two groups (Figures 3A and 3B). The currently uncharacterized gene *obimac0010569* (see Methods S1 for further information) was uniquely expressed in cluster 37, and FISH revealed that these cells were located in the OGL (Figure 4B). This represents an additional population of OGL neurons, beyond the dopaminergic neurons discussed above. On the other hand, a nicotinic acetylcholine receptor (*nachr*) was expressed in clusters 5/6, and these were localized to a broad band in the IGL (Figure 4B). Together, these data demonstrate that the scRNA-seq dopamine+glutamatergic clusters consist of two distinct subtypes, one in the OGL (*obimac0010569*+) and one in the IGL (*nachr*+).

Glutamatergic neurons—We next focused on the subtypes of putative glutamatergic neurons, which include several smaller clusters (33, 34, 28) in addition to a set of larger clusters (29–32) (Figure 2A). Examining genes in the smaller clusters revealed that these contain further subtypes. The first cluster (33) was defined by hedgehog (*hh*), a signaling molecule involved in axon guidance and patterning in the nervous system across many species.[48] FISH showed that *hh*+ *cells* are mainly restricted to a narrow band of neurons in the most superficial OGL, identifying yet another subtype within the OGL (Figure 4C). A second cluster (34) is marked by the voltage-gated calcium channel gamma subunit 5/7 (*cacng*), which FISH demonstrated corresponds to a narrow band of neurons at the border of the IGL and medulla (Figure 4C). Finally, a third cluster (28) specifically expressed a member of the leucine-rich repeat family of cell adhesion molecules (*Irrc15*), which is involved in cell-type-specific synaptic connectivity in fly and mammalian nervous systems.[49] This group was localized to the deeper region of the medulla (Figure 4C). Within the larger set of glutamatergic clusters (29–32), we found that a subset of neurons express vesicular amine transporter 1 (*slc18a1*, or *vat1*), which FISH demonstrated to also be localized to cell bodies in the deeper region of the medulla (Figure 7F). Thus, the glutamatergic neurons primarily constitute a large population of cells within the medulla, along with two subtypes with highly specific sublayer localization within the outer OGL and inner IGL.

Cholinergic neurons—The last neurotransmitter class of cells in the octopus optic lobe is the putative cholinergic neurons. scRNA-seq data revealed a large population of cells (clusters 7–9) and a much smaller population (cluster 35) that both express *vacht*, a marker for cholinergic transmission. FISH for *vacht* showed that cholinergic neurons are located throughout the medulla, with more restricted expression in IGL (Figures 3B and 4D). Moreover, the scRNA-seq data revealed that clusters that comprise this larger population can be delineated based on the expression of family members of two homeobox transcription factors, *nkx2* and *otx*. FISH for these two markers demonstrated that the *nkx2*+ population is located in the IGL and superficial region of the medulla, whereas the *otx*+ population is not expressed in the IGL and, instead, is found throughout the medulla (Figure 4D). In exploring the scRNA-seq data, we found that the *nkx2*+ cluster also expresses a protocadherin (*obimac0026462*), and FISH confirms that *obimac0026462*+ cells are expressed both in the IGL and medulla (Figure 7E).

We observed that neurons in the smaller cholinergic cluster (35) selectively express nitric oxide synthase (*nos*), suggesting that they represent a distinct cell type that uses this neuropeptide as a signaling molecule in addition to acetylcholine. FISH for *nos* revealed these neurons form a narrow sublayer within the superficial to central IGL (Figure 4D). scRNA-seq data show that *nos*+ cells and the glutamatergic *cacng*+ cells, both in the IGL, also express an unidentified gene *obimac0022194* (Methods S1), suggesting that these clusters may have some shared function based on expression of this unidentified gene.

Thus, the cholinergic neurons constitute a large population of the IGL and medullar cells, with distinct anatomical positions defined by a small sublayer of *nkx2*+ cells in the IGL and superficial medulla, *otx*+ cells throughout the medulla, and *nos*+ cells mainly in the superficial IGL.

Orcokinin and octopaminergic neurons—We sought to determine the identity of the two remaining mature neuronal clusters (37 and 4), which were defined by highly specific expression of *orc* and *tyrbh*, respectively (Figures 2A–2C). Cluster 37 did not express any of the neurotransmitter markers we assessed but was demarcated by the expression of the neuropeptide *orc*, and FISH revealed that *orc*+ cells are a sparse, scattered population throughout the deeper region of the medulla (Figure 4E). The final cluster of mature neurons, cluster 4, selectively expressed a number of genes, including *tyrbh*, the synthetic enzyme for octopamine, generally considered to be the invertebrate analog of norepinephrine,[50] which plays a role in arousal and other aspects of behavioral state across species. FISH showed a discrete population of octopaminergic *tyrbh*+ neurons in the OGL (Figure 4F). Among the other genes that were unique to this cluster is a protocadherin family member (*obimac0009200*), which co-expresses with *tyrbh* exclusively in the OGL (Figure 4F), and semaphorin-5 (*sema5*), which is highly expressed in the same region of the OGL, along with some expression throughout the medulla (Figure 4F). Thus, this cluster also expresses genes that serve as adhesion molecules (protocadherin *obimac0009200*) and axon guidance cues (*sema5*) in the visual system of other species.[51,52]

Immature neurons

Finally, we examined the putative immature neuronal clusters, representing 31% of all neurons, which were identified in the scRNA-seq data based on lower expression of *syt* and the absence of mature neurotransmitter markers. We observed that in the U-MAP these clusters were organized into several "arms," suggesting that they may represent discrete populations of developing neurons associated with mature cell types (Figure 2A). One unidentified gene (*obimac0019980*) appears to encompass all nine immature clusters (Figures 5A and 5B; see Methods S1 for further characterization). The immature clusters can then be segregated into three subgroups that are demarcated by complementary expression of genes: a previously unidentified gene *obimac0032150*, which contains a tumor necrosis factor receptor domain (*tnfr*; clusters 18–20 and 27), myoneurin (*mynn*; clusters 22–24), and big brain (*bib*; clusters 25 and 26) (Figures 5A and 5B), all of which are known to play a role in neural development in other species. Since these three genes segregate the population of immature neurons, we used FISH to identify the expression and examine their relationships to the location of the mature cell types described above (Figure 5C).

In the first subgroup, *tnfr* expression appeared in scRNA-seq clusters that are transcriptionally related to mature clusters of cholinergic and glutamatergic neurons (Figures 2A and 5B), which are largely found in the medulla. FISH data for *tnfr* revealed more extensive expression in the medulla, compared with the other putative immature subtypes (Figure 5C). In the second subgroup, scRNA-seq data showed that *mynn*, a zinc-finger protein family member associated with neuromuscular synapse formation in mice,[53] is expressed in a number of clusters in the arms leading to mature cell types for dopaminergic neurons of the OGL (Figures 2A and 5B). Correspondingly, FISH data show that the *mynn*+ cell types border the PL along both the OGL and IGL, together with some cells in the medulla (Figure 5C). In the third subgroup, *bib*, a known neurogenic molecule in *Drosophila*,[54] was expressed in arms leading to the clusters that correspond to the two prominent clusters of dopaminergic+glutamatergic neurons (Figures 2A and 5B). We found *bib* was expressed most strongly, although not exclusively, in cells along the bottom borders of the IGL and OGL (Figure 5C). As mentioned above, all of these subgroup markers are also expressed throughout the medulla, suggesting that they may represent the ongoing migration of immature neurons into the optic lobe. They also have increased expression in stratifications along the borders of the OGL and IGL, raising the possibility that the laminar borders may be an important locus for the incorporation of immature neurons.

Other known developmental genes (Figures 5A and 5D) were expressed in the immature clusters in the scRNA-seq data, and we investigated the expression patterns of three of these genes using FISH: *dschs*, *sox2*, and *dlx* (Figure 5E). We also identified two receptor-ligand pairs that have well established roles in patterning the nervous system in vertebrates and other invertebrates[51,55]—ephrin (*efn*)/Eph receptor (*epha*) and semaphorin-2 (*sema2*)/plexin (*plxna*)—all of which had complementary expression patterns to each other across the scRNA-seq data (Figures 6A and 6B). Graded expression of ephrins and semaphorins and their respective receptors play important roles in establishing large-scale organization during development in other species, including topographic map formation.[51,55] Notably, the ligand-receptor pair *efn* and *epha* were expressed in opposing gradients from superficial

to deep in the optic lobe (Figure 6A). Likewise, *sema2* was expressed in a gradient with strongest expression in the deep medulla, although its potential receptor *plxna* had stronger expression along the borders of the OGL and IGL (Figure 6B).

Together, these data demonstrate that these putative immature neurons are found in distinct anatomical locations with discrete subtypes that can be molecularly defined. Moreover, conserved families of developmental genes, as well as novel cephalopod- or octopus-specific genes, define these subtypes, suggesting the possibility of both evolutionarily conserved and lineage-specific molecular mechanisms for development and function.

Cell-type and sublayer organization of mature neurons in the optic lobe

A driving goal of this project was to identify the "parts list" of the octopus optic lobe and create an integrated model of cell-type organization within their visual system. We therefore incorporated the findings for the mature neurons into a schematic spatial map of the optic lobe (Figures 7A and 7B). Here, we summarize this organization and present multiplexed FISH data for markers within each layer to explicitly demonstrate the sublayer organization.

Outer granular layer—We found four broad groups of cell types within the OGL (Figure 7C). First, a cluster of glutamatergic cells lines the most superficial aspect of the OGL, which also expresses *hh*. Second, one group of neurons from the dopaminergic+glutamatergic clusters is located in the central OGL, marked by an uncharacterized gene *obimac0010569*. Third, we identified a specific subset of octopaminergic neurons that co-expresses *tyrbh* and *pcdhob09200*. Finally, a diverse group of dopaminergic-only neurons spans sublayers of the OGL. This group falls into two major divisions: *six4/5*+ in the central OGL and *dscam*+ in the deep OGL. Notably, the expression of neuropeptides within the *dat*+ group also shows a progression across the depth of the OGL (Figure 7D).

Inner granular layer—We found significant cell-type diversity within the IGL (Figure 7E), consisting of at least four neuronal cell types with distinct sublayer expression patterns. The largest population of cells therein consists of neurons from one of the dopaminergic+glutamatergic clusters, which forms a distinct band as identified by expression of an *nachr*. A small population of cholinergic neurons expressing nos lines the superficial IGL (*obimac0022194*+ is shown in Figure 7E as proxy for *nos*+ cells), whereas a subgroup of glutamatergic neurons (*cacng*) lines the deep IGL. In addition, the *nkx2*+ cholinergic group spans from the IGL into the medulla (Figure 7E includes *obimac0026462* in place of *nkx2*).

Medulla—The medulla comprises a majority of the octopus optic lobe and largely consists of two distinct populations of glutamatergic and cholinergic neurons (Figure 7F), with glutamatergic neurons more prevalent in the central tangential region. Notably, these are intermingled within the cell body "islands" of the medulla, suggesting that, at least at the level of these two large populations, there is no functional segregation across the islands. However, there are apparent distinctions in gene expression across the depth of the medulla. Within the cholinergic group, *nkx2*+ neurons are more superficial, whereas *otx*+ neurons

are located throughout the medulla (Figure 7B). In addition, there is a superficial-to-deep gradient of *vat1* expression that is shared across the cholinergic and glutamatergic neurons (Figure 7F). Finally, there are sparse populations of neurons that express extremely high levels of neuropeptides (Figures 4A and 4E). It is possible that these represent neurons projecting to downstream brain regions where these neuropeptides could play a role in regulating behavioral outputs.[12,16,18,19,56]

DISCUSSION

This study provides a comprehensive molecular description of neural subtype organization of the optic lobe cell types to complement the anatomical descriptions provided by Young.[5] In addition to identifying non-neuronal and developing cells in our dataset, we reveal six major cell classes of mature neurons and a number of subtypes within these that correlate with discrete locations of the optic lobe, uncovering previously unknown cell-type diversity and sublayer organization of the octopus visual system. This study thereby contributes to a recently growing literature on transcriptomics of the cephalopod nervous system[57–59] and lays the basis for both the investigation of the role of distinct cell types in visual processing as well as the development of tools for targeting specific cell classes based on their molecular signatures. In addition to revealing the overall molecular architecture of the optic lobe, a number of the specific findings shown here have implications for elucidating the function and development of the octopus visual system.

We found a wide array of cell types within the OGL, which was previously shown to consist of amacrine cells. Among the three broad classes of amacrine cells in the OGL that Young described,[5] we found at least eight clusters of specific cell types that all have distinct spatial localizations within sublayers of the OGL (Figures 7C and 7D). These cell types are defined by neurotransmitters (largely dopaminergic but also some glutamatergic), neuropeptides, a transcription factor (*six4/5*), an adhesion molecule (*dscam*), and a developmental signaling molecule (*hh*). This array of cell types bears a strong resemblance to the diversity of amacrine cells in the vertebrate retina, where over 60 amacrine cell types have been identified in mice.[60] However, in contrast to vertebrates, where amacrine cells primarily express the inhibitory neurotransmitters GABA or glycine,[61] in the octopus we find that OGL neurons are predominantly dopaminergic. Notably, there is a specific population of dopaminergic amacrine cells in the vertebrate retina,[62] and it has been shown that dendritic tiling in these amacrine cells is dependent on *dscam*,[46] which strikingly is also expressed in a subset of dopaminergic OGL cells here. Moreover, in the vertebrate retina, distinct amacrine cell classes have been linked to a range of specific visual computations.[63] It will be intriguing to see whether similar functions can be assigned to the diversity of cells within the OGL based on the markers we have identified.

We identified a sparse but highly distinct population of neurons in the OGL that express *tyrbh*, the synthetic enzyme for octopamine. In both flies and mice, locomotion and arousal have profound effects on visual processing,[64–66] which, in flies, are mediated by octopamine[67] and, in mice, are mediated in part by norepinephrine.[50,68] Strikingly similar impacts of arousal on visual responses in octopuses were observed in an early study in the octopus EEG,[69] suggesting a potential similar role for this octopaminergic system.

Another notable finding is the delineation of a large population of putative immature neurons within the octopus visual system. *O. bimaculoides* are born capable of feeding and living independently from hatching, relying on a variety of visually guided behaviors.[27,28] Despite this, octopuses continue to grow exponentially in size throughout their lifetime,[70] increasing their mass by approximately 10× every 2 months, including growth of the optic lobes and other brain regions.[71,72] Hence, the finding of such a large population of immature neurons is not surprising, given the octopus's need for neurogenesis in order to support such massive brain growth. It has recently been shown in octopus embryos that neurogenesis occurs outside of the optic lobe, followed by long-distance migration into the optic lobe.[73] Therefore, the immature population we observe likely represents post-mitotic developing neurons that have recently completed migration, rather than a neurogenic population within the optic lobe itself.

In fish and birds, the visual system continues to grow throughout the animal's lifetime by expanding along the periphery in a proliferative marginal zone.[74] By contrast, we find that the immature neuronal population in the octopus is broadly distributed tangentially across the optic lobe, although with potential radial stratification along the borders of the OGL and IGL. Future work examining the ongoing developmental expansion of the optic lobe will be needed to reveal how new neurons coordinate their integration into the fully functioning visual system of the growing octopus.

We found genes associated with both the immature and mature cell types that may contribute to developmental establishment of identity, connectivity, and function, including both conserved (e.g., *hh*, *dscam, nkx, bib*, and *pcdhs*) and novel (*obimac0011980* and *obimac0010569*) genes. We also identified subtypes within immature cell populations that are associated with mature neuronal cell types, suggesting different developmental trajectories and progenitor populations. Another striking developmental finding is the presence of complementary expression of ephrin/Eph receptor and semaphorin/plexin pairs in the optic lobe, suggesting that these receptor-ligand pairs may play a similar role in setting up the spatial organization of the visual system as they do in flies and vertebrates.

Limitations of study

We note that although we have delineated a number of subtypes within the major populations of cells in the octopus optic lobe, there is almost certainly additional diversity to be explored in future studies. Indeed, studies of the vertebrate retina have progressed from the early delineation of five major neuronal cell types to our current understanding of the tremendous diversity within each of these, including 30+ cell types within the retinal ganglion cells alone.[75] This initial description of cell types for the octopus visual system that we provide here can serve as a basis for delving further into such diversity.

In this study, we defined cell types in the octopus visual system based on gene expression and related these cell types to their anatomical location. Future studies that relate these cell types to other aspects of neural identity, including anatomical morphology via single-cell labeling, downstream projection targets based on retrograde tracing, and visual response properties identified through calcium imaging, will be crucial in decoding cephalopod visual function. The molecular mapping we present here provides a roadmap for such studies and

more generally provides a path forward toward cracking the functional, developmental, and evolutionary logic of the cephalopod visual system.

STAR★METHODS

RESOURCE AVAILABILITY

Lead contact—Further information and requests for resources and reagents should be directed to and will be fulfilled by the lead contact, Cristopher Niell (cniell@uoregon.edu).

Materials availability—Probe accession numbers have been deposited at Zenodo and can be accessed using the link provided in the key resources table.

Data and code availability

- Single-cell RNA sequencing data have been deposited at NCBI SRA and GEO and are publicly available. Genome data have been deposited at Zenodo and are publicly available. Accession numbers and DOIs are listed in the key resources table. Microscopy data reported in this paper will be shared by the lead contact upon request.
- All original code has been deposited at Zenodo and is publicly available. DOIs are listed in the key resources table.
- Any additional information required to reanalyze the data reported in this paper is available from the lead contact upon request.

EXPERIMENTAL MODEL AND SUBJECT DETAILS

Octopus bimaculoides were obtained from the Cephalopod Resource Center at the Marine Biology Laboratory (Woods Hole, MA) and from Aquatic Research Consultants (San Pedro, CA). They were kept at the University of Oregon in a closed circulating 250 gallon aquarium system in artificial seawater, and fed daily on a rotating diet of frozen shrimp, crabs, and fish. All husbandry and experimental protocols were in accordance with the EU 2010/63/EU[84] and AAALAC guidelines for the use and care of cephalopods for research.

METHOD DETAILS

Genome sample collection and sequencing—Optic lobe tissue was dissected from an adult female *O. bimaculoides* for whole genome sequencing. Tissue was sent to the University of Oregon Genomics & Cell Characterization Core Facility (GC3F) for DNA extraction and sequencing. High molecular weight genomic DNA was extracted using a Nanobind Tissue Big DNA kit (Circulomics). A Pacific Biosciences standard HiFi library was prepped with a SMRTbell Express Template Prep Kit 2.0. Genomic DNA was sheared at 20kb target size with a Megaruptor 2 instrument (Diagenode). BluePippin size selection (Sage Science) was used to omit the smallest fragments (<10-14kb) to enrich for longer fragments. Two HiFi genomic circular consensus sequencing (CCS) SMRTbell libraries were prepared as input for five HiFi SMRT cells. Single molecule sequencing of both libraries was conducted with a PacBio Sequel II system. After sequencing, data was

imported into SMRT Link to generate 5.8 million HiFi reads with the CCS algorithm and create fastq files.

Four tissues were dissected from 6 week old juvenile octopuses to be used in Iso-Seq sequencing: optic lobe, central brain, retina, and arm. RNA extractions were performed using a RNeasy Plus Mini Kit (QIAGEN). A single bulk non-barcoded SMRTbell Iso-Seq library was prepared according to the manufacturer's protocol (PacBio) by GC3F. A multiplexed Iso-Seq library was sequenced across a single PacBio Sequel II SMRT cell. IsoSeq3 in SMRT Link was used to generate fastq files containing 1.08 million full-length transcripts.

Genome re-assembly and annotation—We used HiFiASM v0.15.5-r352[76] to assemble a contig-level genome with HiFi reads as input and default parameters. After initial assembly, duplications were removed using Purge_dups.[77] Protein-coding genes were annotated using existing bulk RNA sequences and our newly generated Iso-Seq data. Bulk RNA data was aligned to the genome assembly using Hisat v2.2.1[78] and gene predictions were assembled with StringTie v2.1.6[79] using parameters `-c 4 -m 200 -j 3`. All other parameters were set to default. To generate gene predictions with Iso-Seq data, we mapped the full length, non-chimeric reads (FLNC) to the genome using minimap2[80] using parameters `-ax splice -uf -secondary=no -C5 -06, 24 -B4`. After alignment, cDNA_cupcake (https://github.com/Magdoll/cDNA_Cupcake) was used to collapse alignments into transcript models. Unique transcripts with degraded 5' ends were filtered out of the final annotation file with `filter_away_subset.py`. StringTie and cDNA_cupcake annotations were combined using TAMA merge[81] with parameters `-e longest_ends -d merge_dup`.

The transcripts of the resulting gtf were used to run blastp against a Uniprot database and to run hmmer against the pfam database. The resulting hits were used as input for Transdecoder v5.5.0 (https://github.com/TransDecoder/TransDecoder) to predict single best coding regions. The existing mitochondrial genome and annotation were concatenated to the assembled genome and annotation files, respectively. This resulted in a final number of 18,896 gene annotations.

Orthologous relationships between our predicted genes and those of distant species were identified using OrthoFinder v2.5.2.[31] We used default parameters to cluster sequences into orthologue groups using sequences from eight species including *Homo sapiens* (hg38), *Mus musculus* (GCA_000001635.9), *Drosophila melanogaster* (GCA_000001215.4), *Aplysia californica* (GCA_000002 075.2), *Crassostrea gigas* (GCA_902806645.1), *Octopus sinensis* (GCA_006345805.1), and *Sepia pharaonis* (GCA_903632075.3). For orthologue groups that contained fewer than four genes, a tree was not generated. These genes were manually annotated using NCBI BLAST[32,85] to assign putative identity based on homology to deposited sequences in other species. Identities for putative neuropeptides (*flri, fmrf, lxgkr*, and *pxfv*) were assigned based on repeats within their predicted protein sequences.

Cell dissociation for scRNA-seq—Animals used for scRNA-seq were 6 week old juveniles with mantle lengths of 6.5mm-9.0mm. *O. bimaculoides* optic lobes were dissected

on ice in Leibovitz-15 medium (Gibco) supplemented with 400mM NaCl, 10mM KCl, 15mM Hepes, 200 U/mL penicillin, and 0.2 mg/mL streptomycin. Single cell dissociation was performed by incubating tissue in papain (1 mg/ml; Worthington Biochemical Co) plus 1% DNase (10mg/ml in HBSS) in supplemented L-15 medium for 10 min at RT. The cells/tissue were gently pipetted up and down several times to dissociate large chunks. The cells/tissue were incubated for another 10 min at RT, pipetted up and down several times, and quenched in wash solution containing 2.5M glucose, 5mM Hepes, and 5% FBS in CMFSS (12mM Hepes, 435mM NaCl, 10.7mM KCl, 21mM Na2HPO4, 16.6mM glucose). Dissociated cells were passed through a 40 μM cell strainer (Fisherbrand), washed again, and resuspended in L-15 medium. A final sample cell concentration of 2000 cells per microliter, as determined on a BioRad TC20 cell counter, was used for cDNA library preparation. Dissociated samples were prepared in tandem, on the same day.

Single-cell cDNA library preparation—Sample preparation for two biological replicates was performed by the University of Oregon Genomics and Cell Characterization core facility (https://gc3f.uoregon.edu/). Dissociated cells were run on a 10X Chromium platform using 10x v.3 chemistry targeting 10,000 cells. The resulting cDNA libraries were amplified with 11 cycles of PCR and sequenced on either an Illumina Hi-seq or an Illumina Next-seq.

RNA Fluorescence In Situ Hybridization—Tissue collection for RNA fluorescence in situ hybridization consisted of juvenile octopuses (~4-6 weeks in age, 7mm in mantle length), which were first anesthetized in 4% EtOH in Artificial Seawater prior to fixation. Anesthetic replaced the seawater in the octopus' home chamber, and the chamber was placed on ice until the octopus was no longer ventilating or responsive. The mantle and arms were removed, leaving the central brain complex which was immediately placed into 10% Neutral Buffered Formalin. The brains were fixed for 24 hours at room temperature before being processed and embedded in paraffin and sectioned into 7um slices.

Custom probes were designed and ordered through Advanced Cell Diagnostics (ACDBio) (Hayward, CA). We followed the protocol available for ACDBio RNAscope,[86] with minor changes to optimize it for use in paraffin-embedded octopus tissue. Briefly, we first removed the paraffin through baking, xylenes, and ethanol washes. We then fixed the tissue for 30 minutes in formalin at room temperature before dehydrating the tissue with an ethanol series. We proceeded with hybridization and target retrieval: 10min pre-treatment of H_2O_2, 12min target retrieval in a pressure cooker, and protease plus for 25min at 40C. Slides incubated with probes for 2 hours before going into washes and 5X SSC overnight. On Day 2, we proceeded with amplification and used the appropriate HRPs and opal dyes before adding the HRP block. For multiple probes, additional HRP conjugates were added in a series-wise manner (HRP, opal dyes, block) before slides were mounted with DAPI and ProLong Gold Antifade.

Microscopy—Slides were imaged on the Leica SP8 confocal at 40x. Confocal images were scanned in a z-stack at 1um steps (2um steps for Figure S3) and were tiled. The resulting tiling merged image was then processed in FIJI.[83] The maximum intensity projection was generally taken across 8 planes (13 for Figure 1, 9 for Figure 6, 5 for Figure

S3). When applicable, background subtraction was applied with a rolling ball radius of 100 pixels.

QUANTIFICATION AND STATISTICAL ANALYSIS

Cluster analysis—The sequencing data were analyzed using the 10X Cell Ranger pipeline, version 3.1.0 (Zheng et al.)[30] and the Seurat (version 3.1.4; Satija et al.[82]) software package for R, version 4.1.2, using standard quality control, normalization, and analysis steps.

Briefly, raw data from each biological replicate were read into R, with a minimum threshold of 3 cells and 500 genes. After visualizing the raw reads, genes, and mitochondrial percentage, we set thresholds of counts between 1000 and 20000, features above 600 genes, and less than 6 percent of mitochondrial content for downstream processing.

To correct for batch effects between our replicates, we followed guidelines for normalization and integration provided by Stuart et al.,[29] and Hafemeister and Satija[87] respectively. We selected integration features within each dataset and applied SCTransform normalization before integrating the datasets based on Canonical Correlation Analysis.[29] For generating cell type clusters, we ran all of the following analyses on the “integrated” assay, but performed differential expression analysis on the “SCT” assay. Following standard downstream processing steps, we ran principal component analysis and UMAP on 25 dimensions. We ran FindNeighbors (dims 1:25) and FindClusters (resolution 0.85). We then generated a dendrogram and renumbered clusters based on this output. We identified the top differentially expressed markers and used these data to identify and subset the putative neurons. We also excluded one cluster from the rest of the analyses due to low number of transcripts and genes, suggesting this cluster did not represent real cellular expression. We re-ran UMAP on the subset of neurons and used this output for visualization and further cell type identification based on top differentially expressed markers. All UMAPs, including feature plots, are shown with datasets that are downsampled to 500 cells for visualization purposes. However, all dot plots show gene expression for full datasets. Feature plots for Figure 2B are shown with a min.cutoff of 0 and a max.cutoff of 1, except for *syt* which has a min.cutoff of 1 and a max.cutoff of 2. Feature plots for Figures 3 and 4 are shown with a min.cutoff of 0 and a max.cutoff of 4. Feature plots for Figures 5 and 6 are shown with a min.cutoff of 0 and a max.cutoff of 2.

Supplementary Material

Refer to Web version on PubMed Central for supplementary material.

ACKNOWLEDGMENTS

We thank members of the Niell, Miller, and Kern labs for helpful discussions and comments on the manuscript. We acknowledge support from the University of Oregon Genomics & Cell Characterization Core Facility and Imaging Core Facility. We thank Leah DeBlander for assistance with slide-scanner imaging and Poh-Keng Loi for performing tissue sectioning. This work was supported by National Institutes of Health R01NS118466-01 (C.M.N.), R01NS118466-01S1 (C.M.N. and J.O.S.-C.), and R01HG010774 (A.D.K.); Office of Naval Research N00014-21-1-2426 (C.M.N.); University of Oregon Renee James Seed grant (A.C.M. and C.M.N.); and National Science Foundation Graduate Research Fellowship grant no. 1842486 (G.C.C.).

REFERENCES

1. Williamson R, and Chrachri A (2004). Cephalopod neural networks. Neurosignals. 13, 87–98. [PubMed: 15004427]
2. Budelmann BU (1995). The cephalopod nervous system: what evolution has made of the molluscan design. In The Nervous System of Invertebrates: An Evolutionary and Comparative Approach, Breidbach O, and Kutsch W, eds. (Springer), pp. 115–138.
3. Nixon M, and Young JZ (2003). The Brains and Lives of Cephalopods (Oxford University Press).
4. Young JZ (1961). Learning and discrimination in the octopus. Biol. Rev. Camb. Philos. Soc 36, 32–96. [PubMed: 13787471]
5. Young JZ (1962). The optic lobes of Octopus vulgaris. Phil. Trans. R. Soc. Lond. B 245, 19–58.
6. Wells MJ (1962). Brain and Behaviour in Cephalopods (Stanford University Press).
7. Chiao CC, and Hanlon RT (2001). Cuttlefish camouflage: visual perception of size, contrast and number of white squares on artificial checkerboard substrata initiates disruptive coloration. J. Exp. Biol 204, 2119–2125. [PubMed: 11441053]
8. Hanlon RT, and Messenger JB (2018). Cephalopod Behaviour (Cambridge University Press).
9. Ogura A, Ikeo K, and Gojobori T (2004). Comparative analysis of gene expression for convergent evolution of camera eye between octopus and human. Genome Res. 14, 1555–1561. [PubMed: 15289475]
10. Young JZ (1962). The retina of cephalopods and its degeneration After optic nerve section. Phil. Trans. R. Soc. Lond. B 245, 1–18.
11. Yamamoto T, Tasaki K, Sugawara Y, and Tonosaki A (1965). Fine structure of the octopus retina. J. Cell Biol 25, 345–359. [PubMed: 14287185]
12. Young JZ (1971). The Anatomy of the Nervous System of Octopus Vulgaris (Oxford University Press).
13. Messenger JB (1981). Comparative physiology of vision in molluscs. Comparative Physiology and Evolution of Vision in Invertebrates (Springer), pp. 93–200.
14. Bullock TH, and Budelmann BU (1991). Sensory evoked potentials in unanesthetized unrestrained cuttlefish: a new preparation for brain physiology in cephalopods. J. Comp. Physiol. A 168, 141–150. [PubMed: 2033566]
15. Young JZ (1979). The nervous system of loligo: V. The vertical lobe complex. Phil. Trans. R. Soc. Lond. B 285, 311–354.
16. Chichery R, and Chanelet J (1976). Motor and behavioral responses obtained by stimulation with chronic electrodes of the optic lobe of Sepia officinalis. Brain Res. 105, 525–532. [PubMed: 1260459]
17. Shigeno S, Andrews PLR, Ponte G, and Fiorito G (2018). Cephalopod brains: an overview of current knowledge to facilitate comparison with vertebrates. Front. Physiol 9, 952. [PubMed: 30079030]
18. Young JZ (1974). The central nervous system of Loligo. I. The optic lobe. Philos. Trans. R. Soc. Lond. B Biol. Sci 267, 263–302. [PubMed: 4132206]
19. Boycott BB, and Young JZ (1961). The functional organization of the brain of the cuttlefish Sepia officinalis. Proc. R. Soc. Lond. B 153, 503–534.
20. Saidel WM (1982). Connections of the octopus optic lobe: an HRP study. J. Comp. Neurol 206, 346–358. [PubMed: 7096632]
21. Liu Y-C, Liu TH, Su C-H, and Chiao C-C (2017). Neural organization of the optic lobe changes steadily from late embryonic stage to adulthood in cuttlefish Sepia pharaonis. Front. Physiol 8, 538. [PubMed: 28798695]
22. y Cajal SR (1930). Contribución Conocimiento Retina y centros ópticos de los cefalópodos (Unión Internacional de Ciencias Biológicas, Comité Español).
23. Konstantinides N, Kapuralin K, Fadil C, Barboza L, Satija R, and Desplan C (2018). Phenotypic convergence: distinct transcription factors regulate common terminal features. Cell 174, 622–635.e13. e13. [PubMed: 29909983]

24. Peng Y-R, Shekhar K, Yan W, Herrmann D, Sappington A, Bryman GS, van Zyl T, Do MTH, Regev A, and Sanes JR (2019). Molecular classification and comparative taxonomics of foveal and peripheral cells in primate retina. Cell 176, 1222–1237.e22. e22. [PubMed: 30712875]
25. Macosko EZ, Basu A, Satija R, Nemesh J, Shekhar K, Goldman M, Tirosh I, Bialas AR, Kamitaki N, Martersteck EM, et al. (2015). Highly parallel genome-wide expression profiling of individual cells using nanoliter droplets. Cell 161, 1202–1214. [PubMed: 26000488]
26. Tasic B, Menon V, Nguyen TN, Kim TK, Jarsky T, Yao Z, Levi B, Gray LT, Sorensen SA, Dolbeare T, et al. (2016). Adult mouse cortical cell taxonomy revealed by single cell transcriptomics. Nat. Neurosci 19, 335–346. [PubMed: 26727548]
27. Solorzano Y, Viana MT, López LM, Correa JG, True CC, and Rosas C (2009). Response of newly hatched Octopus bimaculoides fed enriched artemia salina: growth performance, ontogeny of the digestive enzyme and tissue amino acid content. Aquaculture 289, 84–90.
28. Hanlon RT, and Forsythe JW (1985). Advances in the laboratory culture of octopuses for biomedical research. Lab. Anim. Sci 35, 33–40. [PubMed: 3981958]
29. Stuart T, Butler A, Hoffman P, Hafemeister C, Papalexi E, Mauck WM 3rd, Hao Y, Stoeckius M, Smibert P, and Satija R (2019). Comprehensive integration of single-cell data. Cell 177, 1888–1902.e21. e21. [PubMed: 31178118]
30. Zheng GXY, Terry JM, Belgrader P, Ryvkin P, Bent ZW, Wilson R, Ziraldo SB, Wheeler TD, McDermott GP, Zhu J, et al. (2017). Massively parallel digital transcriptional profiling of single cells. Nat. Commun 8, 14049. [PubMed: 28091601]
31. Emms DM, and Kelly S (2019). OrthoFinder: phylogenetic orthology inference for comparative genomics. Genome Biol. 20, 238. [PubMed: 31727128]
32. Altschul SF, Gish W, Miller W, Myers EW, and Lipman DJ (1990). Basic local alignment search tool. J. Mol. Biol 215, 403–410. [PubMed: 2231712]
33. Deryckere A, and Seuntjens E (2018). The cephalopod large brain enigma: are conserved mechanisms of stem cell expansion the key? Front. Physiol 9, 1160. [PubMed: 30246785]
34. Messenger JB (1996). Neurotransmitters of cephalopods. Invertebrate Neuroscience 2, 95–114.
35. Bröer A, Tietze N, Kowalczuk S, Chubb S, Munzinger M, Bak LK, and Bröer S (2006). The orphan transporter v7-3 (slc6a15) is a Na+-dependent neutral amino acid transporter (B0AT2). Biochem. J. 393, 421–430. [PubMed: 16185194]
36. Juorio AV, and Molinoff PB (1971). Distribution of octopamine in nervous tissues of Octopus vulgaris. Br. J. Pharmacol 43, 438P–439P.
37. Cornwell CJ, Messenger JB, and Williamson R (1993). Distribution of GABA-like immunoreactivity in the octopus brain. Brain Res. 621, 353–357. [PubMed: 8242349]
38. Seo HC, Curtiss J, Mlodzik M, and Fjose A (1999). Six class homeobox genes in Drosophila belong to three distinct families and are involved in head development. Mech. Dev 83, 127–139. [PubMed: 10381573]
39. Kumar JP (2009). The sine oculis homeobox (six) family of transcription factors as regulators of development and disease. Cell. Mol. Life Sci 66, 565–583. [PubMed: 18989625]
40. Weasner BP, Anderson J, and Kumar JP (2004). The eye specification network in Drosophila. Proc. Indian Natl. Sci. Acad. B Biol. Sci B70, 517–530. [PubMed: 25580038]
41. Kawakami K, Sato S, Ozaki H, and Ikeda K (2000). Six family genes–structure and function as transcription factors and their roles in development. Bioessays. 22, 616–626. [PubMed: 10878574]
42. Krajniak KG (2013). Invertebrate FMRFamide related peptides. Protein Pept. Lett 20, 647–670. [PubMed: 22630125]
43. Zatylny-Gaudin C, and Favrel P (2014). Diversity of the RFamide peptide family in mollusks. Front. Endocrinol. 5, 178.
44. Loi P, Saunders R, Young D, and Tublitz N (1996). Peptidergic regulation of chromatophore function in the European cuttlefish Sepia officinalis. J. Exp. Biol 199, 1177–1187. [PubMed: 9319020]
45. Loi PK, and Tublitz NJ (2000). Roles of glutamate and FMRFamide-related peptides at the chromatophore neuromuscular junction in the cuttlefish, Sepia officinalis. J. Comp. Neurol 420, 499–511. [PubMed: 10805923]

46. Fuerst PG, Koizumi A, Masland RH, and Burgess RW (2008). Neurite arborization and mosaic spacing in the mouse retina require DSCAM. Nature 451, 470–474. [PubMed: 18216855]
47. Yamagata M, and Sanes JR (2008). Dscam and Sidekick proteins direct lamina-specific synaptic connections in vertebrate retina. Nature 451, 465–469. [PubMed: 18216854]
48. Yang C, Qi Y, and Sun Z (2021). The role of sonic hedgehog pathway in the development of the central nervous system and aging-related neurodegenerative diseases. Front. Mol. Biosci 8, 711710. [PubMed: 34307464]
49. de Wit J, Hong W, Luo L, and Ghosh A (2011). Role of leucine-rich repeat proteins in the development and function of neural circuits. Annu. Rev. Cell Dev. Biol 27, 697–729. [PubMed: 21740233]
50. Roeder T. (1999). Octopamine in invertebrates. Prog. Neurobiol 59, 533–561. [PubMed: 10515667]
51. Pasterkamp RJ (2012). Getting neural circuits into shape with semaphorins. Nat. Rev. Neurosci 13, 605–618. [PubMed: 22895477]
52. Peek SL, Mah KM, and Weiner JA (2017). Regulation of neural circuit formation by protocadherins. Cell. Mol. Life Sci 74, 4133–4157. [PubMed: 28631008]
53. Cifuentes-Diaz C, Bitoun M, Goudou D, Seddiqi N, Romero N, Rieger F, Perin J-P, and Alliel PM (2004). Neuromuscular expression of the BTB/POZ and zinc finger protein myoneurin. Muscle Nerve 29, 59–65. [PubMed: 14694499]
54. Rao Y, Bodmer R, Jan LY, and Jan YN (1992). The big brain gene of Drosophila functions to control the number of neuronal precursors in the peripheral nervous system. Development 116, 31–40. [PubMed: 1483394]
55. Wilkinson DG (2001). Multiple roles of EPH receptors and ephrins in neural development. Nat. Rev. Neurosci 2, 155–164. [PubMed: 11256076]
56. Liu T-H, and Chiao C-C (2017). Mosaic organization of body pattern control in the optic lobe of squids. J. Neurosci 37, 768–780. [PubMed: 28123014]
57. Styfhals R, Zolotarov G, Hulselmans G, Spanier KI, Poovathingal S, Elagoz AM, Deryckere A, Rajewsky N, Ponte G, Fiorito G, et al. (2022). Cell type diversity in a developing octopus brain. Preprint at bioRxiv. 10.1101/2022.01.24.477459.
58. Duruz J, Sprecher M, Kaldun JC, Alsoudy A, Tschanz-Lischer H, van Geest G, Nicholson P, Bruggmann R, and Sprecher SG (2022). Molecular characterization of cell types in the squid Loligo vulgaris. Preprint at bioRxiv. 10.1101/2022.03.28.485983.
59. Gavriouchkina D, Tan Y, Ziadi-Künzli F, Hasegawa Y, Piovani L, Zhang L, Sugimoto C, Luscombe N, Marlétaz F, and Rokhsar DS (2022). A single-cell atlas of bobtail squid visual and nervous system highlights molecular principles of convergent evolution. Preprint at bioRxiv. 10.1101/2022.05.26.490366.
60. Yan W, Laboulaye MA,Tran NM, Whitney IE, Benhar I, and Sanes JR (2020). Mouse retinal cell atlas: molecular identification of over sixty amacrine cell types. J. Neurosci 40, 5177–5195. [PubMed: 32457074]
61. Diamond JS (2017). Inhibitory interneurons in the retina: types, circuitry, and function. Annu. Rev. Vis. Sci 3, 1–24. [PubMed: 28617659]
62. Witkovsky P. (2004). Dopamine and retinal function. Doc. Ophthalmol 108, 17–40. [PubMed: 15104164]
63. Masland RH (2012). The tasks of amacrine cells. Vis. Neurosci 29, 3–9. [PubMed: 22416289]
64. Niell CM, and Stryker MP (2010). Modulation of visual responses by behavioral state in mouse visual cortex. Neuron 65, 472–479. [PubMed: 20188652]
65. Chiappe ME, Seelig JD, Reiser MB, and Jayaraman V (2010). Walking modulates speed sensitivity in Drosophila motion vision. Curr. Biol 20, 1470–1475. [PubMed: 20655222]
66. Vinck M, Batista-Brito R, Knoblich U, and Cardin JA (2015). Arousal and locomotion make distinct contributions to cortical activity patterns and visual encoding. Neuron 86, 740–754. [PubMed: 25892300]
67. Suver MP, Mamiya A, and Dickinson MH (2012). Octopamine neurons mediate flight-induced modulation of visual processing in Drosophila. Curr. Biol 22, 2294–2302. [PubMed: 23142045]

68. Polack PO, Friedman J, and Golshani P (2013). Cellular mechanisms of brain state-dependent gain modulation in visual cortex. Nat. Neurosci 16, 1331–1339. [PubMed: 23872595]
69. Boycott BB, Lettvin JY, Maturana HR, and Wall PD (1965). Octopus optic responses. Exp. Neurol 12, 247–256. [PubMed: 14314553]
70. Forsythe JW, and Hanlon RT (1988). Effect of temperature on laboratory growth, reproduction and life span of Octopus bimaculoides. Mar. Biol 98, 369–379.
71. Yamazaki A, Yoshida M, and Uematsu K (2002). Post-hatching development of the brain in Octopus ocellatus. Zoolog. Sci 19, 763–771. [PubMed: 12149577]
72. Kerbl A, Handschuh S, Nödl MT, Metscher B, Walzl M, and Wanninger A (2013). Micro-CT in cephalopod research: investigating the internal anatomy of a sepiolid squid using a non-destructive technique with special focus on the ganglionic system. J. Exp. Mar. Biol. Ecol 447, 140–148.
73. Deryckere A, Styfhals R, Elagoz AM, Maes GE, and Seuntjens E (2021). Identification of neural progenitor cells and their progeny reveals long distance migration in the developing octopus brain. eLife 10, e69161. [PubMed: 34425939]
74. Fernald RD (1990). Teleost vision: seeing while growing. J. Exp. Zool. Suppl 5, 167–180. [PubMed: 1982493]
75. Sanes JR, and Masland RH (2015). The types of retinal ganglion cells: current status and implications for neuronal classification. Annu. Rev. Neurosci 38, 221–246. [PubMed: 25897874]
76. Cheng H, Concepcion GT, Feng X, Zhang H, and Li H (2021). Haplotype-resolved de novo assembly using phased assembly graphs with hifiasm. Nat. Methods 18, 170–175. [PubMed: 33526886]
77. Guan D, McCarthy SA, Wood J, Howe K, Wang Y, and Durbin R (2020). Identifying and removing haplotypic duplication in primary genome assemblies. Bioinformatics 36, 2896–2898. [PubMed: 31971576]
78. Kim D, Paggi JM, Park C, Bennett C, and Salzberg SL (2019). Graph-based genome alignment and genotyping with HISAT2 and HISAT-genotype. Nat. Biotechnol 37, 907–915. [PubMed: 31375807]
79. Kovaka S, Zimin AV, Pertea GM, Razaghi R, Salzberg SL, and Pertea M (2019). Transcriptome assembly from long-read RNA-seq alignments with StringTie2. Genome Biol. 20, 278. [PubMed: 31842956]
80. Li H. (2018). Minimap2: pairwise alignment for nucleotide sequences. Bioinformatics 34, 3094–3100. [PubMed: 29750242]
81. Kuo RI, Cheng Y, Zhang R, Brown JWS, Smith J, Archibald AL, and Burt DW (2020). Illuminating the dark side of the human transcriptome with long read transcript sequencing. BMC Genomics 21, 751. [PubMed: 33126848]
82. Satija R, Farrell JA, Gennert D, Schier AF, and Regev A (2015). Spatial reconstruction of single-cell gene expression data. Nat. Biotechnol 33, 495–502. [PubMed: 25867923]
83. Schindelin J, Arganda-Carreras I, Frise E, Kaynig V, Longair M, Pietzsch T, Preibisch S, Rueden C, Saalfeld S, Schmid B, et al. (2012). Fiji: an open-source platform for biological-image analysis. Nat. Methods 9, 676–682. [PubMed: 22743772]
84. Fiorito G, Affuso A, Basil J, Cole A, de Girolamo P, D'Angelo L, Dickel L, Gestal C, Grasso F, Kuba M, et al. (2015). Guidelines for the Care and Welfare of Cephalopods in Research -A consensus based on an initiative by CephRes, FELASA and the Boyd Group. Lab. Anim 49, 1–90.
85. Altschul SF, Madden TL, Schäffer AA, Zhang J, Zhang Z, Miller W, and Lipman DJ (1997). Gapped BLAST and PSI-BLAST: a new generation of protein database search programs. Nucleic Acids Res. 25, 3389–3402. [PubMed: 9254694]
86. Wang F, Flanagan J, Su N, Wang L-C, Bui S, Nielson A,Wu X, Vo H-T, Ma X-J, and Luo Y (2012). RNAscope: a novel in situ RNA analysis platform for formalin-fixed, paraffin-embedded tissues. J. Mol. Diagn 14, 22–29. [PubMed: 22166544]
87. Hafemeister C, and Satija R (2019). Normalization and variance stabilization of single-cell RNA-seq data using regularized negative binomial regression. Genome Biol. 20, 296. [PubMed: 31870423]

Highlights

- scRNA-seq and FISH identified molecular cell types in the octopus visual system
- Cell types defined by functional and developmental markers show sublayer organization
- Immature neurons form transcriptional subgroups that correspond to mature cell types
- This atlas is a basis for studying visual function and development in cephalopods

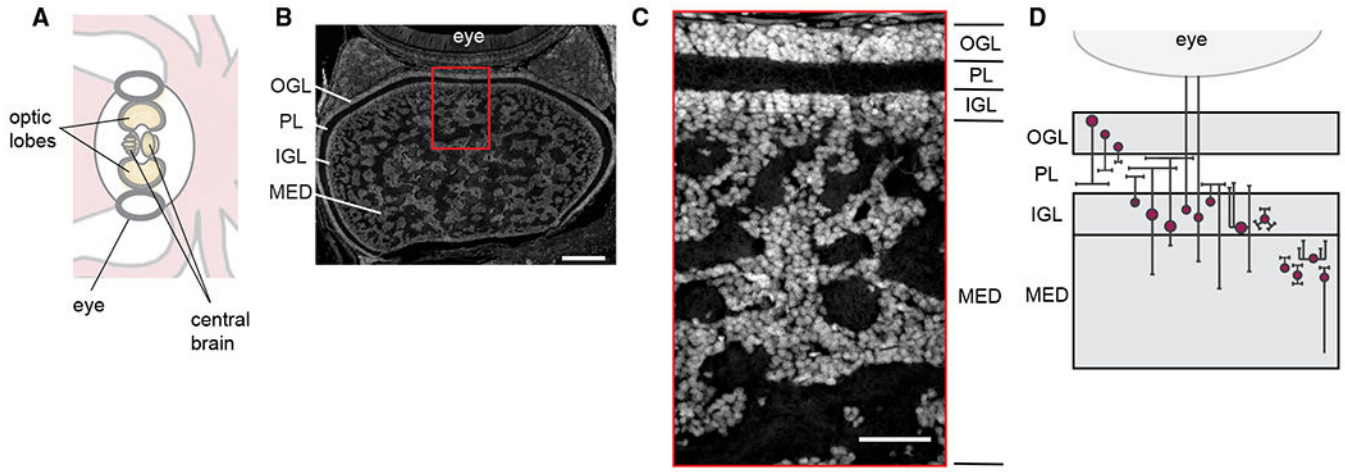

Figure 1. Laminar organization of *O.bimaculoides* optic lobes

(A) Schematic showing the octopus central nervous system, which includes optic lobes behind each eye and the central brain in between.

(B) Overview of one optic lobe and eye. Nuclei are stained with DAPI. Scale bar, 200 μm. Red box denotes the region shown in (C). OGL, outer granular layer; PL, plexiform layer; IGL, inner granular layer; and MED, medulla.

(C) Laminar organization of the optic lobe demonstrated by nuclear staining of a cross-section. Scale bar, 50 μm.

(D) Schematic of the anatomical organization of the visual system, in terms of neuronal morphologies, adapted from the study conducted by Young.[5]

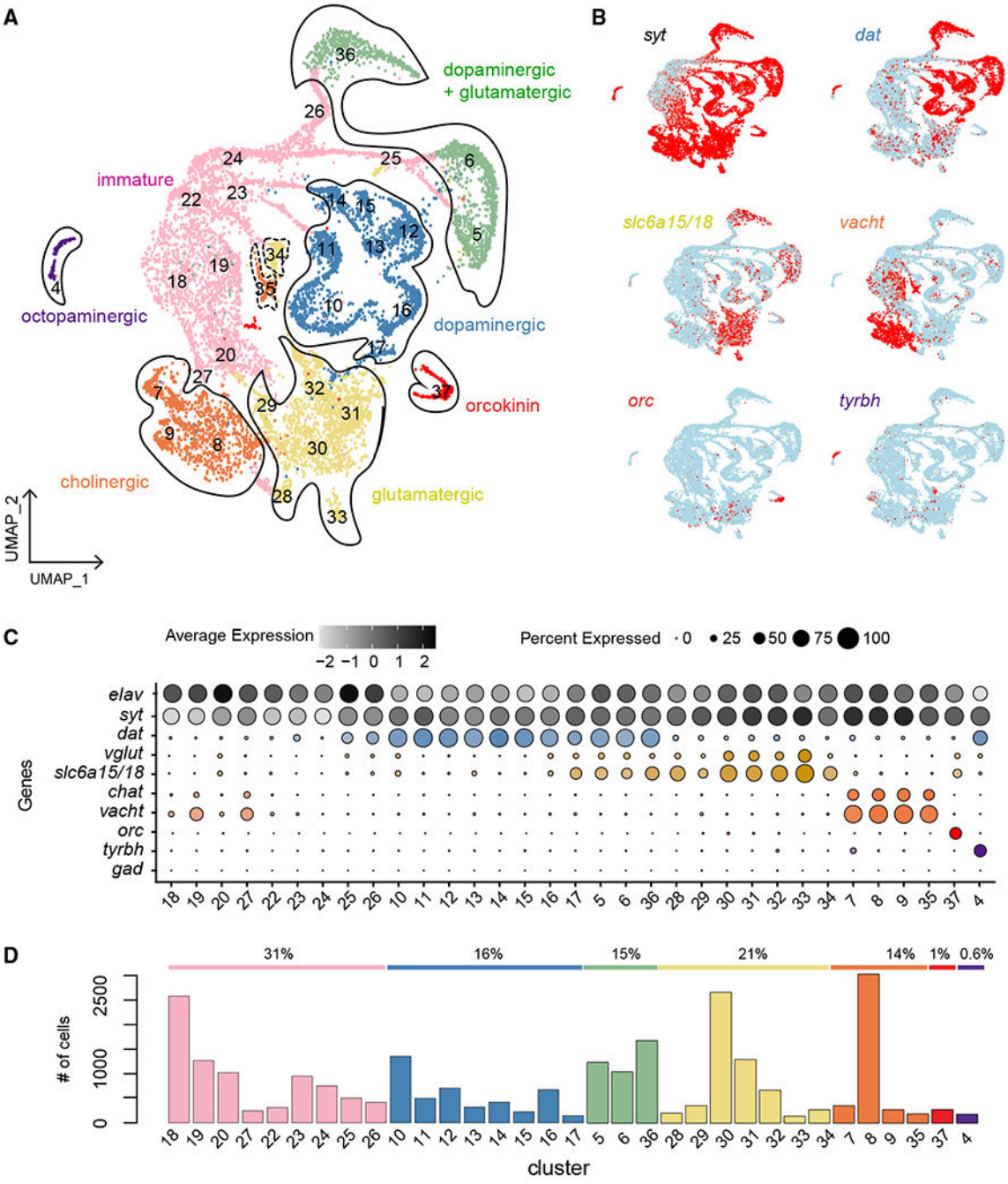

Figure 2. scRNA-seq reveals six major neuronal classes

(A) UMAP of putative neuronal clusters. A total of 33 clusters are color-coded based on major cell classes.

(B) Feature plots showing expression patterns of marker genes for neurons (*syt*) and neurotransmitter phenotypes (dopaminergic cells [*dat*], glutamatergic cells [*slc6a15/18*], cholinergic cells [*vacht*], orcokinin cells [*orc*], and octopaminergic cells [*tyrbh*]).

(C) Dot plot of markers delineating molecular cell classes.

(D) Bar graph indicating total number of cells in each cluster as colored in (A) as well as the relative proportion of each cell class across the entire population of neurons in the optic lobe.

See also Figures S1–S4 and Tables S1 and S2.

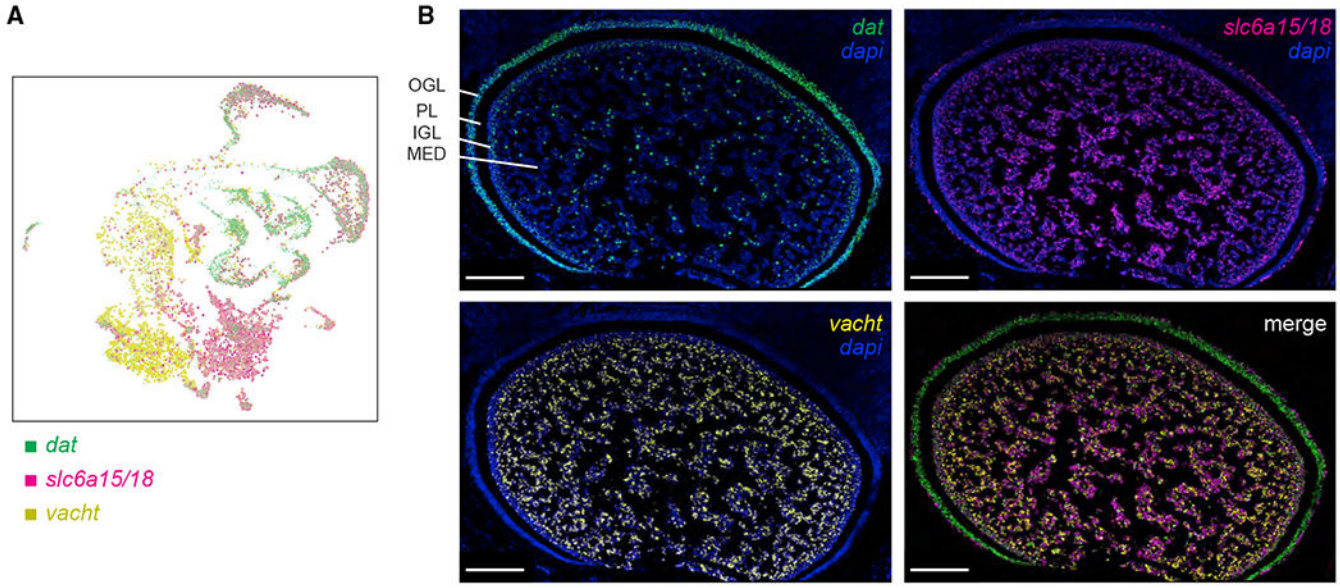

Figure 3. Neurotransmitter usage divides the majority of cells into four large populations

(A) UMAP of overlay of *dat*, *slc6a15/18*, and *vacht* expression.

(B) FISH of *dat*, *slc6a15/18*, and *vacht*, with nuclei stained in DAPI, and merged FISH of the three neurotransmitter-related genes. Scale bars, 100 μm. Here and below, merged images are shown without DAPI to emphasize relative expression patterns.

See also Figure S4 and Table S2.

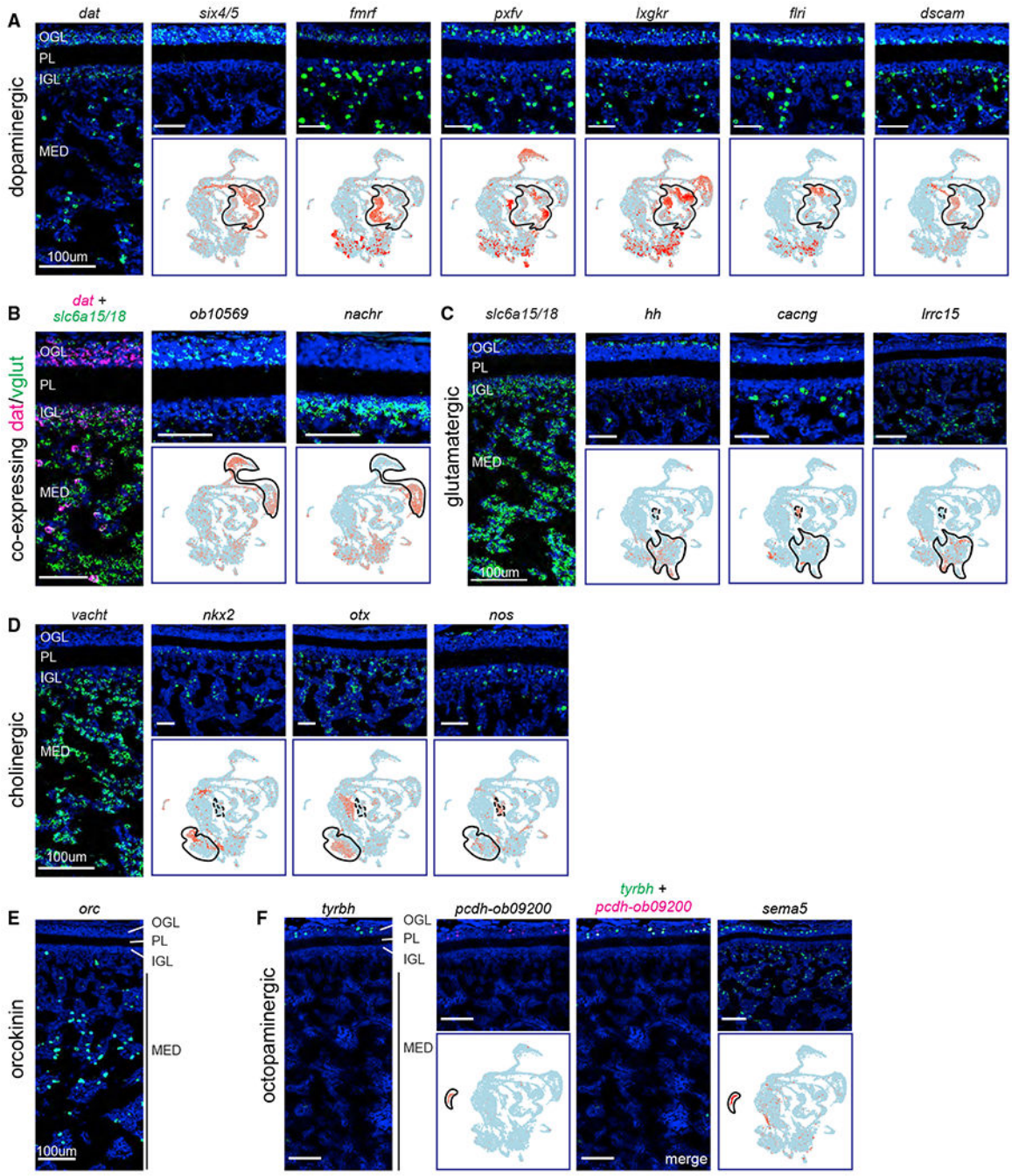

Figure 4. Anatomical organization of major cell classes and subtypes based on scRNA-seq and FISH

(A) Dopaminergic neuron organization. *dat*+ cells are divided into two major subtypes based on the additional differential expression of either *six4/5*+ or *fmrf*+, depicted through FISH and scRNA-seq feature plots. Corresponding cell classes are outlined in black on the feature plots and nuclei are stained with DAPI (blue). All scale bars 50 μm unless otherwise noted.

(B) Neuron organization for scRNA-seq clusters that co-express *dat* and *slc6a15/18*.

(C) Glutamatergic subtype neuron organization.

(D) Cholinergic subtype neuron organization.

(E) Orcokinin neuron organization.

(F) Octopaminergic neuron organization. From left to right: *tyrbh*, *pcdh-obimac0009200*, double FISH of *tyrbh* and *pcdh-obimac0009200*, and a single FISH of *sema5*.

See also Table S2 and Methods S1.

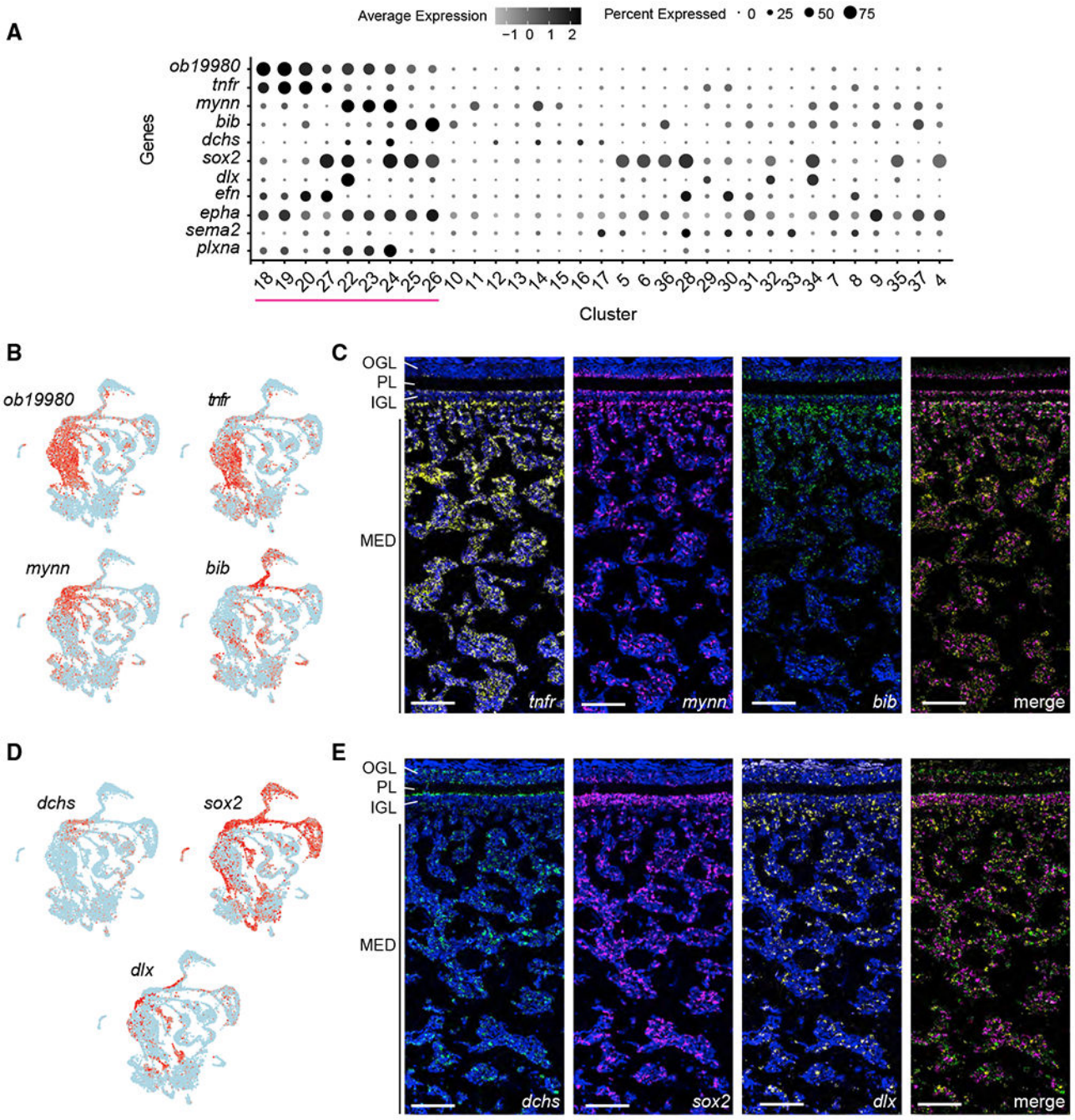

Figure 5. Gene expression and spatial organization of putative immature neurons

(A) Dot plot of genes expressed in immature neurons, with magenta line highlighting immature clusters.

(B) Feature plot of uncharacterized cephalopod-specific gene *obimac0019980*, which demarcates the putative immature neuronal clusters, as well as three genes that define distinct subgroups within the immature neurons: *tnfr*, *mynn*, and *bib*.

(C) FISH of the genes delineating the three subgroups shown in (B), including a merged FISH. Throughout this figure, DAPI is shown in blue on individual FISHs. Scale bars, 100 μm.

(D) Feature plots of additional markers from development-related gene family trees demonstrating further cell-type diversity.

(E) FISH showing anatomical organization of the genes shown in (D) including a merged FISH.

See also Table S2 and Methods S1.

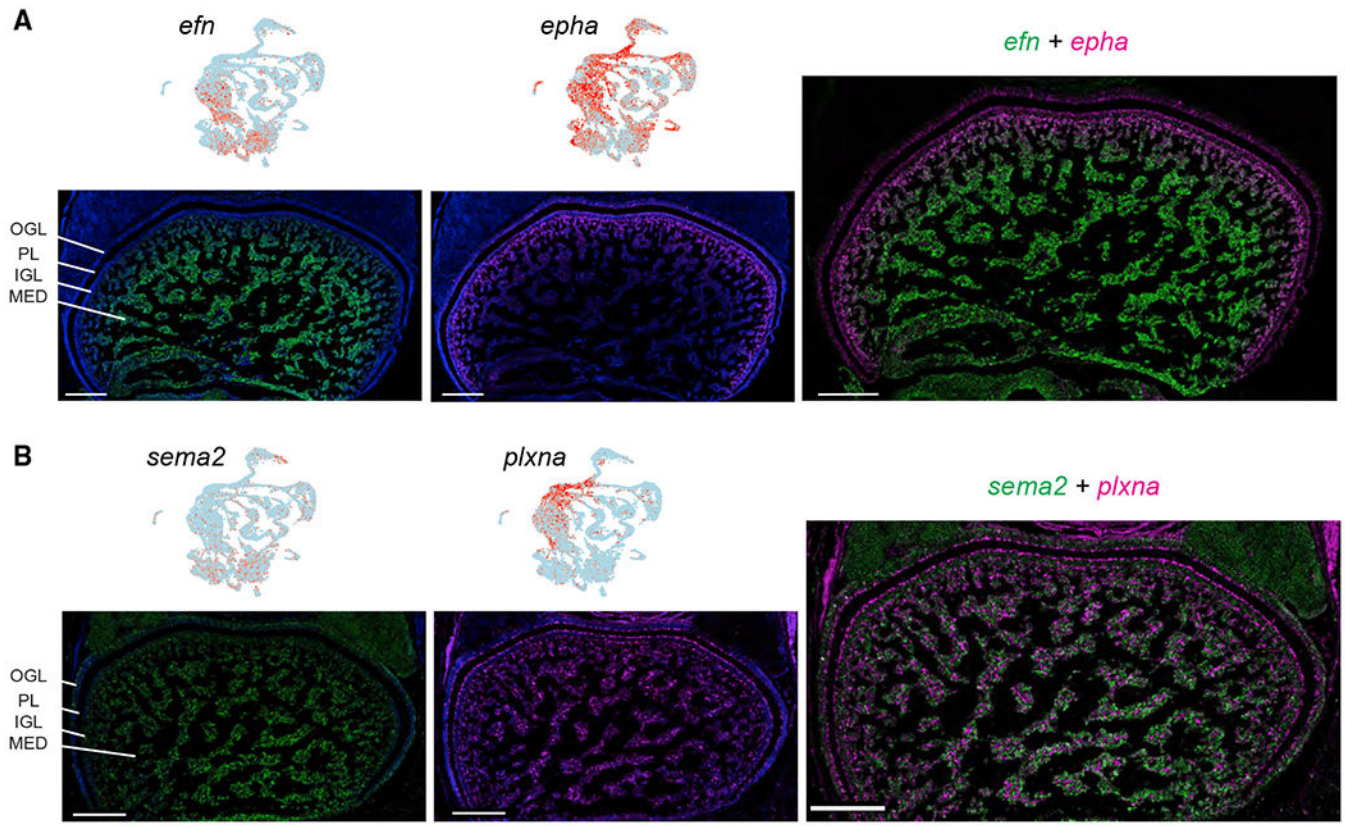

Figure 6. Expression of conserved patterning molecules

(A) Feature plots showing complementary scRNA-seq expression of an ephrin/Eph-receptor pair. FISH for these genes shows corresponding gradients of expression.

(B) Feature plots showing scRNA-seq complementary expression of a semaphorin/plexin pair. FISH for these genes shows corresponding spatial patterns of expression.

Nuclei are stained with DAPI in blue. Scale bars, 200 μm.

See also Table S2.

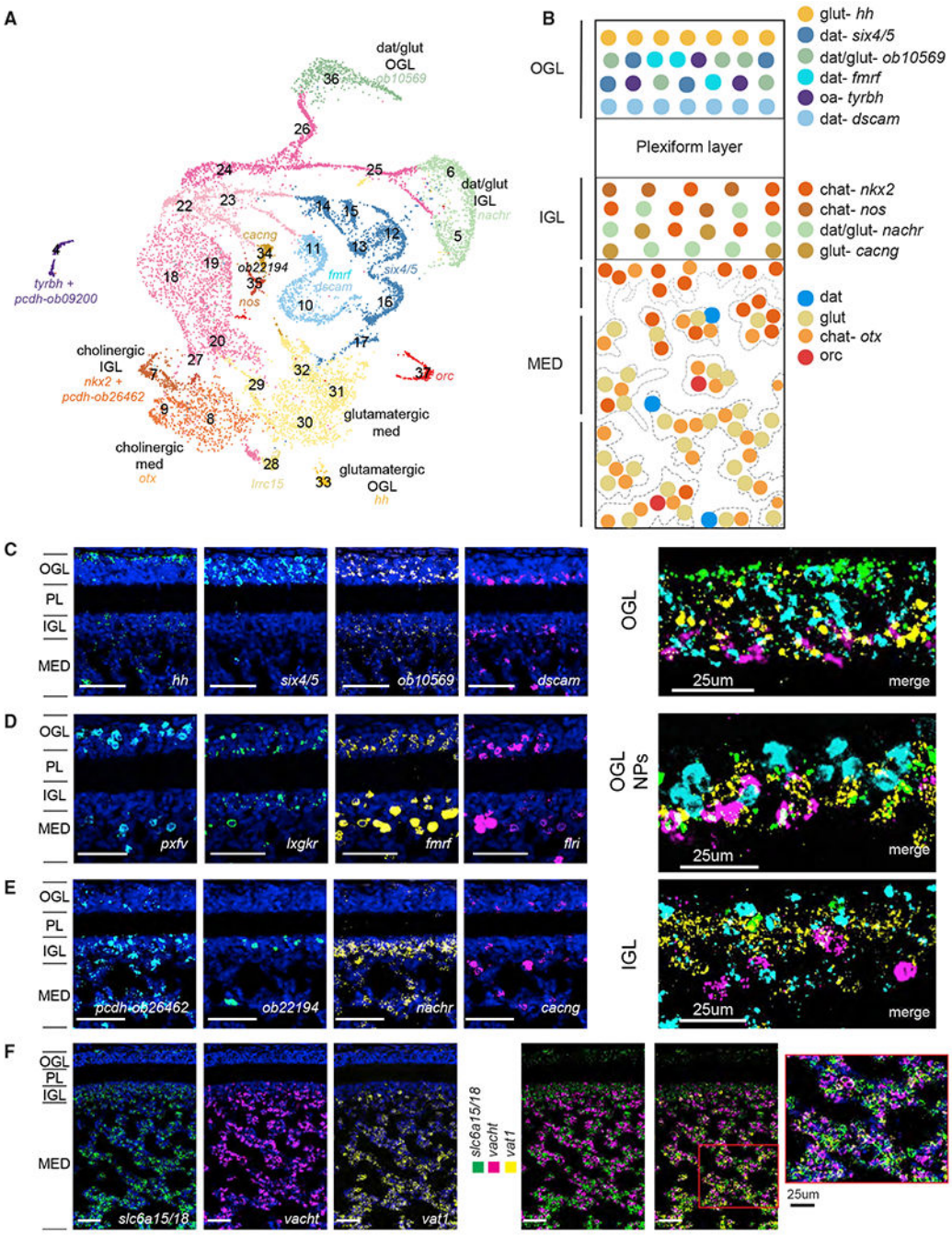

Figure 7. Summary of mature neuronal architecture

(A) UMAP showing cell subtypes in each neuronal class, along with annotation of spatial localization within the optic lobe.

(B) Schematic of cell-type organization of the optic lobe. Genes defining subtypes are color-coordinated to match their clusters in (A).

(C) FISH showing sublayers of the OGL. Sublayers of OGL are demarcated from most superficial to deepest in order by expression of *hh*, *six4/5*, unidentified gene

obimac0010569, and *dscam*. Throughout this figure, nuclei are stained with DAPI in blue. Unless otherwise noted, scale bars, 50 μm.

(D) FISH of neuropeptides that subdivide dopaminergic neurons in the OGL. In order from most superficial to the deepest: *pxvf*, *lxgkr*, *fmrf*, and *flri*.

(E) FISH showing sublayers of IGL based on expression of *pcdh-obimac0026462*, unidentified gene *obimac0022194*, *nachr*, and *cacng*.

(F) FISH showing organization of the medulla. The medulla has cell body islands with non-overlapping expression of populations of glutamatergic (*slc6a15/18*+) and cholinergic (*vacht*+) neurons, whereas *vat1* is expressed in a subset of medulla cell bodies.

See also Table S2 and Methods S1.

KEY RESOURCES TABLE

REAGENT or RESOURCE	SOURCE	IDENTIFIER
Biological samples		
Adult *Octopus bimaculoides*	Aquatic Research Consultants (San Pedro, CA)	N/A
Juvenile *Octopus bimaculoides*	Cephalopod Resource Center at the Marine Biology Laboratory (Woods Hole, MA)	N/A
Chemicals, peptides, and recombinant proteins		
RNAscope O.bimaculoides gene probes	ACDBio	Zenodo: 10.5281/zenodo.6211860
Leibovitz-15	Gibco	CAT NO: 21083027
NaCl	Fisher Scientific	CAT NO: S271-1
KCl	Alfa Aesar	CAT NO: 11595
Hepes	Fisher Scientific	CAT NO: BP310-100
Penicillin-Streptomycin	Sigma	CAT NO: P4333-100ML
Papain	Worthington Biochemical Co	CAT NO: LK003178
Dnase	Worthington Biochemical Co	CAT NO: LK003170
HBSS	Fisher Scientific	CAT NO: 14025092
Glucose	Tokyo Chemical Industry	CAT NO: G0048
FBS	Gibco	CAT NO: 16-140-063
CMFSS	N/A	N/A
Na_2HPO_4	Sigma	CAT NO: S0876-1KG
EtOH	Deacon Laboratories	CAT NO: 2701
10% Neutral Buffered Formalin	Fisher Scientific	CAT NO: 23-245684
Xylenes	Aqua Solution	SKU# X7502-500ML
Opal dye 520	Akoya Sciences	CAT NO: FP1487001KT
Opal dye 570	Akoya Sciences	CAT NO: FP1488001KT
Opal dye 620	Akoya Sciences	CAT NO: FP1495001KT
Opal dye 690	Akoya Sciences	CAT NO: FP1497001KT
ProLong Gold Antifade	Invitrogen	CAT NO: P36930
20X SSC	Invitrogen	CAT NO: 15-557-044
Critical commercial assays		
Nanobind Tissue Big DNA kit	Circulomics	CAT NO: SKU 102-302-100 (previously NB-900-701-01)
SMRTbell Express Template Prep Kit 2.0	Pacific Biosciences	PN 100-938-900
SMRTbell Enzyme Cleanup Kit	Pacific Biosciences	PN 101-746-400
Proximo Animal Hi-C v4.0 Kit	Phase Genomics	N/A
RNeasy Plus Mini Kit	Qiagen	CAT NO: 74134
RNAscope 4-Plex Ancillary Kit for Multiplex Fluorescent Kit v2	ACDBio	CAT NO: 323120

REAGENT or RESOURCE	SOURCE	IDENTIFIER
RNAscope Multiplex Fluorescent Detection Kit v2	ACDBio	CAT NO: 323110
RNAscope Multiplex Fluorescence Reagent Kit v2	ACDBio	CAT NO: 323100
Deposited data		
RNA sequencing reads	This paper	SRA: PRJNA854179; GEO: GSE212528
Genome assembly	This paper	Zenodo: 10.5281/zenodo.6211860
Genome annotation	This paper	Zenodo: 10.5281/zenodo.6211860
OrthoFinder gene trees	This paper	Zenodo: 10.5281/zenodo.6211860
Cell Ranger output for single-cell RNA sequencing	This paper	Zenodo: 10.5281/zenodo.6211860
Rmd file for O. bimaculoides optic lobe cell type analysis	This paper	Zenodo: 10.5281/zenodo.6211860
Probe sequences for FISH	This paper	Zenodo: 10.5281/zenodo.6211860
Software and algorithms		
HiFiasm (version 0.15.5-r352)	Cheng et al.[76]	https://github.com/chhylp123/hifiasm
Purge_dups (version 1.2.5)	Guan et al.[77]	https://github.com/dfguan/purge_dups
Hisat2 (version 2.2.1)	Kim et al.[78]	https://daehwankimlab.github.io/hisat2/
StringTie (version 2.1.6)	Kovaka et al. [79]	http://ccb.jhu.edu/software/stringtie/index.shtml?t=manual
Minimap2 (version 2.24-r1122)	Li[80]	https://github.com/lh3/minimap2
cDNA_cupcake (version v25.2.0)	https://github.com/Magdoll/cDNA_Cupcake	N/A
TAMA merge (version commit df0d741f6932a2cd845ca324bbbca1464c2139e7)	Kuo et al. [81]	https://github.com/GenomeRIK/tama/wiki/Tama-Merge
Transdecoder (version 5.5.0)	https://github.com/TransDecoder/TransDecoder	N/A
OrthoFinder (version 2.5.2)	Emms and Kelly[31]	https://github.com/davidemms/OrthoFinder
Cell Ranger (version 3.1.0)	Zheng et al.[30]	N/A
R (version 4.1.2)	https://www.r-project.org/	N/A
Seurat (version 3.1.4)	Satija et al.[82]	https://satijalab.org/seurat/
FIJI	Schindelin et al.[83]	https://imagej.net/software/fiji/